Factoring Dynamic Bayesian Networks Based on Structural Observability

Indranil Roychoudhury, Gautam Biswas, and Xenofon Koutsoukos

Abstract— **Dynamic Bayesian Networks (DBNs) provide a systematic framework for robust online monitoring of dynamic systems. This paper presents an approach for increasing the efficiency of online estimation by partitioning a system DBN into a set of smaller factors, such that estimation algorithms can be applied to each factor independently. Our factoring scheme is based on the analysis of structural observability of the dynamic system. We establish the theoretical background for structural observability and derive an algorithm for generating the factors using structural observability analysis. We present experimental results to demonstrate the effectiveness of our factoring approach for accurate estimation of system behavior.**

I. Introduction

Robust online monitoring of safety-critical systems is essential for their safe and efficient operation. Dynamic Bayesian Networks (DBNs) [1] provide a systematic method for modeling the dynamics of complex systems in the presence of noise and sensor inaccuracies. A DBN is a directed acyclic graph that compactly models a dynamic system. The nodes of a DBN represent random variables, and directed links capture the causal relations between these variables at a time point, and across consecutive time steps. DBN-based state-estimation methods apply to nonlinear systems and arbitrary probability distributions, and hence, generalize Kalman filtering approaches [1]. However, robust estimation algorithms using DBNs are exponential in the number of state variables, and for nonlinear systems and non-Gaussian noise models, analytic, closed form, exact estimation methods may not exist. Approximate estimation algorithms (e.g., Boyen-Koller (BK) algorithm [2], particle filtering (PF) [3]) are therefore used for state estimation. However, these approaches require large computational resources as well.

This paper proposes a solution to improving the efficiency of DBN state estimation by factoring the system model into multiple non-overlapping factors, by expressing some of the state variables as algebraic functions of measurements converted to system inputs. As a result, the across-time links directed towards these state variables are replaced by intra-time links from the measurements. This makes some of the state variables in the generated factors conditionally independent from the state variables in other factors, given the measurements. Hence, the state estimation in one factor becomes independent of the other factors, and the state estimation for the individual factors can be carried out separately, thus increasing the overall computational efficiency.

Estimation of state variables from the system measurements works only if the system is *observable*. The traditional schemes for analyzing observability apply to linear systems and depend on the numerical values of the system parameters. This work employs the bond graph modeling paradigm to establish *structural observability* [4], [5]. Structural observability does not depend on the numerical values of the system parameters, and applies to nonlinear systems where the nonlinearities are in the system components, and not in the system structure. In this paper, we apply structural observability analysis to establish a factoring scheme for DBNs that allow for correct estimation of system state even when each factor is executed independent of the others.

II. Previous Work

Distributed decentralized extended Kalman filters (DDEKF) [6] represent an approach for subdividing the estimation problem into smaller subproblems. However, in DDEKFs, each local component requires both measurements and state variable estimate from other components to correctly estimate its states. As a result, inaccuracies in one component can affect the estimation in other components. In our estimation approach, the random variables in a factor are conditionally independent of those in all other factors, given a subset of the measurements. Hence, failures in individual factors do not affect the estimates of the other factors as long as the required measurements are available.

The BK algorithm, presented in [2], creates the individual factors by eliminating causal links between weakly interacting subsystems. The belief state derived from the individual factors is an approximation of the true belief state, but the error in approximation is bounded. However, the bounds may not be sufficiently precise for online monitoring of mission-critical systems. Heuristic techniques for automatically decomposing a DBN into factors are presented in [7]. This approach results in lower estimation errors, but the computed factored belief state is still an approximation. The Factored Particle filtering (FPF) scheme [8] further reduces estimation errors by applying the PF scheme to the BK factored inference approach. Our estimation approach uses the PF scheme for inference using DBNs and preserves the overall system dynamics in the factored form. Hence, we produce accurate state estimates efficiently.

This work was supported by the National Science Foundation under Grant CNS-0615214 and NASA NRA NNX07AD12A.

Indranil Roychoudhury is with SGT, Inc. at NASA Ames Research Center, Moffett Field, CA 94035, USA. Email:indranil.roychoudhury@nasa.gov

Gautam Biswas and Xenofon Koutsoukos are with the Institute for Software Integrated Systems, and the Department of Electrical Engineering and Computer Science, Vanderbilt University, Nashville, TN 37235, USA. Email:{gautam.biswas, xenofon.koutsoukos}@vanderbilt.edu

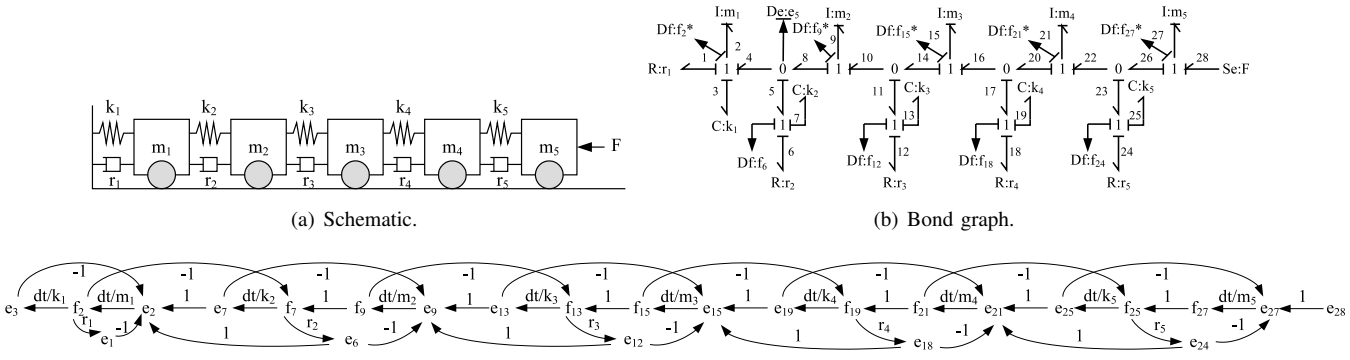

(a) Schematic.

(b) Bond graph.

(c) Temporal causal graph.

Fig. 1. Spring-mass-damper system models.

III. State Estimation Using DBNs

A. Dynamic Bayesian Networks

A DBN is represented as $D = (\mathbf{X}, \mathbf{U}, \mathbf{Y})$, where $\mathbf{X}$, $\mathbf{U}$, and $\mathbf{Y}$ are sets of stochastic random variables that denote (unknown) state variables, system input variables, and measured variables of the dynamic system, respectively [1]. Graphically, a DBN is a two-slice Bayesian network, representing a snapshot of system behavior in two consecutive time slices, t and $t+1$. Each DBN time-slice represents the Markov process observation model, $P(\mathbf{Y}_t|\mathbf{X}_t, \mathbf{U}_t)$ derived from causal links $X_t \rightarrow Y_t$ and $U_t \rightarrow Y_t$, where $X \in \mathbf{X}$, $Y \in \mathbf{Y}$, $U \in \mathbf{U}$, and subscript t represents time. Similarly, across-time causal links $X_t \rightarrow X_{t+1}$, $X_t \rightarrow X'_{t+1}$, and $U_t \rightarrow X_{t+1}$, where $X' \in \mathbf{X}$, represent the Markov state-transition model, $P(\mathbf{X}_{t+1}|\mathbf{X}_t, \mathbf{U}_t)$. Fig. 2(a) shows the DBN for a spring-mass-damper (SMD) system (shown in Fig. 1(a), and described below), where thick-lined circles denote state variables, thin-lined circles denote observed variables, and squares denote input variables.

B. Deriving DBNs of Physical Systems

We systematically derive the DBN for a physical system from the system's temporal causal graph (TCG) [9], which, in turn, is derived from the system BG [10]. The BG modeling paradigm provides a framework for domain-independent, energy-based, topological modeling of physical processes. The nodes of a BG include energy storage (capacitors, C, and inertias, I), dissipation (resistors, R), transformation (gyrators, GY, and transformers, TF), source (effort sources, Se, and flow sources, Sf), and sensor (effort detectors, De, and flow detectors, Df) elements. Nonlinear systems are modeled by parameter values that are functions of other system variables. *Bonds*, drawn as half arrows, with associated effort, e, and flow, f, variables, represent the power interaction pathways between the bond graph elements, such that the product, $e \cdot f$, defines the power transferred through the bond. 0- and 1-junctions represent idealized connections for lossless energy transfer between two or more BG elements.

Fig. 1(b) shows the BG of a tenth-order SMD system (shown in Fig. 1(a)). In the mechanical domain, I elements represent masses, C elements represent springs, R elements represent dampers, flows represent velocities (e.g., f_2 denotes the velocity of mass m_1, and f_6 denotes the relative velocity between masses m_2 and m_1), and efforts represent forces, (e.g, e_3 denotes the force on spring k_1). We assume that the velocities f_2^*, f_6, f_9^*, f_{12}, f_{15}^*, f_{18}, f_{21}^*, f_{24}, f_{27}^*, and the force, e_5, are the available sensors (measurements) in this SMD model[1]. The force, $e_{28} = F$, impressed upon mass m_5 is a system input. In this system, the BG parameters are assumed to be constant.

The TCG, an enhanced signal flow diagram, captures the causal and temporal relations between system variables through directed *edges* and their *labels* [10]. *Causality* establishes the cause and effect relationships between the e and f variables of the bonds determined by constraints imposed by the incident BG elements. Some BG elements, such as the energy storage elements, can either impose *integral* (preferred) or *derivative* causality. The sequential causal assignment procedure (SCAP) systematically assigns the causality in a BG [11]. The nodes in a TCG correspond to the e or f variables of the system BG model. Fig. 1(c) shows the TCG for the SMD system[2]. The direction of a TCG edge and its label are based on causality. For example, for a C element in integral causality, $e = (1/C) \int f dt$, and hence the TCG edge directed from the flow to the effort has a label dt/C, with dt denoting a temporal relationship between f and e. For a C element in derivative causality, the TCG edge is directed from the effort to the flow, since $f = Cde/dt$, and has a label C/dt. In a BG, the state variables are the *displacement*, q (where $\dot{q} = f$), and *momentum*, p (where $\dot{p} = e$), of C and I elements in integral causality, respectively.

The system DBN is constructed from its TCG using the method outlined in [9]. After we identify the TCG nodes, $\mathbf{N}$, which include all state variables, measured variables, and system inputs; for each $N \in \mathbf{N}$, we instantiate nodes N_t and N_{t+1} in the consecutive time slices of the DBN. Then, for every pair of variables, $N, N' \in \mathbf{N}$ that are algebraically related, causal links $N_t \rightarrow N'_t$ and $N_{t+1} \rightarrow N'_{t+1}$ are constructed in each DBN time slice. For every pair of

[1]If a state variable N is directly measured, we denote the corresponding sensor reading as N^*, e.g., f_2^* is the measured value of f_2.

[2]For clarity, the measured variables are not shown in the TCG.

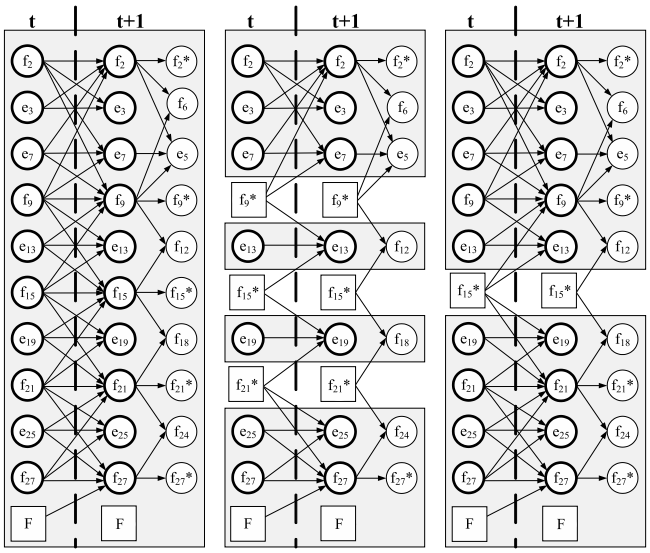

(a) Full DBN. (b) 4-factored DBN. (c) 2-factored DBN.

Fig. 2. Factorings of the Spring-mass-damper DBN.

variables, $N, N' \in \mathbf{N}$ having an integrating relation (i.e., a delay), the across-time $N_t \rightarrow N'_{t+1}$ link is added to the DBN. Fig. 2(a) shows the DBN for the SMD system.

C. Using Particle Filtering for State Estimation

The general iterative solution of the DBN state estimation problem is $P(\mathbf{X}_{t+1}|\mathbf{Y}_{0:t+1}) = \alpha P(\mathbf{Y}_{t+1}|\mathbf{X}_{t+1}, \mathbf{U}_t) \times \sum_{\mathbf{X}_t} P(\mathbf{X}_{t+1}|\mathbf{X}_t, \mathbf{U}_t) P(\mathbf{X}_t|\mathbf{Y}_{0:t})$, where $\mathbf{Y}_{0:t}$ denotes measurement readings from time 0 to t, and α is the normalizing factor [1]. In this work, we choose PF as our iterative algorithm for DBN state estimation [3]. PF is a sequential Monte Carlo method that approximates the belief state of a system using a weighted set of samples, or *particles* [12]. The value of each particle describes a possible system state, and its weight denotes the likelihood of the observed measurements given this particle's value. As more observations are obtained, each particle is moved stochastically to a new state, and the weight of each particle is readjusted to reflect the likelihood of that observation given the particle's new state.

D. Structural Observability

To ensure accurate tracking of system behavior for diagnosis, the system must be *observable*, i.e., all its state variables can be correctly determined given the available measurements [13]. We describe a more general property of structural observability, and show how this property holds for nonlinear systems. Consider the basic state-space formulation of a n^{th}-order LTI system: $\dot{\mathbf{X}} = \mathcal{A}\mathbf{X} + \mathcal{B}\mathbf{U}$, and $\mathbf{Y} = \mathcal{C}\mathbf{X} + \mathcal{D}\mathbf{U}$, where $\mathbf{X}$, $\mathbf{U}$, and $\mathbf{Y}$ represent the state, input and measurement variables of the system, respectively, and $\mathcal{A}$, $\mathcal{B}$, $\mathcal{C}$, and $\mathcal{D}$ are matrices with appropriate dimensions.

Definition 1. [13] (Observability). A system is *observable* if its initial state variables, $\mathbf{X}_{t_0}$, at time t_0, can be derived from the knowledge of inputs, $\mathbf{U}_{t_0:t_f}$, and outputs, $\mathbf{Y}_{t_0:t_f}$, in the time interval $[t_0, t_f]$, where t_f is the current time.

A system is observable if its observablity matrix, $\mathcal{O} = \left[\mathcal{C}^t, (\mathcal{C}\mathcal{A})^t, \ldots, (\mathcal{C}\mathcal{A}^{n-1})^t\right]^t$ is of full rank, i.e., *rank*$(\mathcal{O}) = n$. Therefore, system observability is a function of the numeric values of the system parameters. An alternative approach defines observability as a function of the system structure [4], [5]. This notion of *structural observability* holds for a class of structurally equivalent systems. If a system is structurally observable, but its $\mathcal{O}$ matrix is not of full rank, i.e., $rank(\mathcal{O}) < n$, the full rank can be restored by perturbing the values of elements of its $\mathcal{A}$ and $\mathcal{C}$ matrices [4]. The structural observability properties of a system can be determined by analyzing its BG [4]. The notion of *structural rank* (*struct-rank*) is central to this analysis.

Definition 2. [4] (Structural Rank). *Structural rank* of a matrix is defined as the maximal rank of this matrix as a function of its free parameters, taking into account the relations between parameters.

For example, *struct-rank* $\left(\begin{bmatrix} -R/L_1 & R/L_2 \\ R/L_1 & -R/L_2 \end{bmatrix}\right) = 1$, since the second row of the matrix is linearly dependent on the first row.

Given the BG model of a system with matrices $\mathcal{A}$, $\mathcal{B}$, $\mathcal{C}$, and $\mathcal{D}$, the system is structurally observable iff [4]:

1) every dynamical element of the BG in integral causality is causally connected to a measurement sensor, and
2) *struct-rank*$([\mathcal{A}^t\ \mathcal{C}^t]^t) = n$, where n is the number of state variables in the system.

Intuitively, condition 1 is satisfied if for each independent decoupled subsystem, at least one dynamical element in integral causality is causally connected to a measurement.

Condition 2 is satisfied if the causality of *every* I and C element initially in integral causality can be inverted to produce a valid derivative causality assignment for the BG model. In some situations, De and Df elements may have to be changed into their dual form to assign consistent derivative causality to the BG. This procedure for manipulating the BG to directly determine the structural rank of matrix $[\mathcal{A}^t\ \mathcal{C}^t]^t$ has been presented as the following result in [4]:

$$\textit{struct-rank}\left(\begin{bmatrix} \mathcal{A} \\ \mathcal{C} \end{bmatrix}\right) = \textit{rank}\left(\begin{bmatrix} S_{11} \\ S_{21} \\ S_{31} \end{bmatrix}\right) = n - t_d, \qquad (1)$$

where S_{11}, S_{21}, and S_{31} are components of the junction structure matrix (introduced below); and t_d is the number of dynamical elements remaining in integral causality after (*i*) derivative causality assignment is performed, and (*ii*) the maximal number of output detectors are dualized to eliminate as many storage elements in integral causality as possible. Hence, if every I and C element initially in integral causality can be assigned derivative causality, we get $t_d = 0$, and condition 2 above is satisfied. Structural analysis of a BG model can help determine the structural rank of $[\mathcal{A}^t\ \mathcal{C}^t]^t$ since the structure of the BG plays a crucial role in determining the state-space equations of a system, as we show below.

The *junction structure* (see Fig. 3) represents the structure of a BG and contains information about the BG elements,

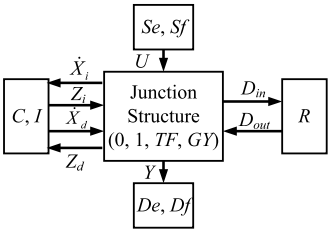

Fig. 3. Junction Structure.

and how they are interconnected (this is independent of the numerical values of the parameters). The junction structure can be represented using a *junction structure matrix*, S [5]:

$$\begin{bmatrix} \dot{X}_i \\ D_{in} \\ Y \end{bmatrix} = \begin{bmatrix} S_{11} & S_{12} & S_{13} & S_{14} \\ S_{21} & 0 & S_{23} & S_{24} \\ S_{31} & 0 & S_{33} & S_{34} \end{bmatrix} \begin{bmatrix} Z_i \\ \dot{X}_d \\ D_{out} \\ U \end{bmatrix} \quad (2)$$

where the state vector X_i is composed of energy variables (p and q variables) of I and C elements in integral causality (denoted by subscript i), X_d is the vector of energy variables of I and C elements in derivative causality, Y is the vector of system outputs, and U is the vector of system inputs. D_{in} and D_{out} represent the effort or flow variables imposed upon, and imposed by the R elements, respectively, as shown in Fig. 3. Z_i and Z_d denote the vector of flow (respectively, effort) variables of I (respectively, C) elements in integral and derivative causality, respectively.

Basic laws associated with each component produce $D_{out} = LD_{in}$, and $Z_i = F_i X_i$, where L is a diagonal matrix composed of R and $\frac{1}{R}$ coefficients, and F_i is composed of $\frac{1}{I}$ and $\frac{1}{C}$ coefficients. We assume that the original system models do not have I and C elements in derivative causality, as these elements can be usually collapsed into one "equivalent" inductor or capacitor in integral causality. Hence, in this work, we assume that X_d and Z_d do not exist. Therefore, state-space equations of a system can be derived from its corresponding junction structure matrix as follows [4]: $\dot{X}_i = \mathcal{A}X_i + \mathcal{B}U$ and $Y = \mathcal{C}X_i + \mathcal{D}U$, with

$$\begin{aligned} \mathcal{A} &= [S_{11} + S_{13}L(I - S_{23}L)^{-1}S_{21}]F_i \\ \mathcal{B} &= [S_{14} + S_{13}L(I - S_{23}L)^{-1}S_{24}] \\ \mathcal{C} &= [S_{31} + S_{33}L(I - S_{23}L)^{-1}S_{21}]F_i \\ \mathcal{D} &= [S_{34} + S_{33}L(I - S_{23}L)^{-1}S_{24}]. \end{aligned}$$

To prove Eqn. (1), let us assume $X_i = [X_{i_1}^t X_{i_2}^t]^t$, with $X_{i_1} \in \mathbb{R}^{n-m}$, $X_{i_2} \in \mathbb{R}^m$, and *rank*$([S_{11}\ S_{12}]) = m$. Given the junction structure matrix shown in Eqn. (2), inverting the causality of as many I and C elements from integral to derivative causality, while retaining consistent causality assignments in the BG model without having to dualize the output detectors yields a new junction structure:

$$\begin{bmatrix} \dot{X}_{i_1} \\ Z_{i_2} \\ D_{in} \\ Y \end{bmatrix} = \begin{bmatrix} 0 & M_1 & 0 & M_2 \\ M_3 & M_4 & M_5 & M_6 \\ 0 & M_7 & M_8 & M_9 \\ M_{10} & M_{11} & M_{12} & M_{13} \end{bmatrix} \begin{bmatrix} Z_{i_1} \\ \dot{X}_{i_2} \\ D_{out} \\ U \end{bmatrix} \quad (3)$$

where X_{i_1} represents state variables that correspond to I and C elements remaining in integral causality after derivative causality assignment is performed, and X_{i_2} represents state variables that correspond to those I and C elements that are assigned derivative causality.

Dualizing of detectors implies decomposing $Y = [Y_1^t\ Y_2^t]^t$, $Y \in \mathcal{R}^p$, and $Y_1 \in \mathcal{R}^{p*}$, where Y_1 represents the sensors that are dualized, and Y_2 represents those sensors that are not dualized. After dualizing the sensors, a new junction structure is built as follows [4]:

$$\begin{bmatrix} \dot{X}_i \\ Z \\ D_{in}^* \\ Y_2 \end{bmatrix} = \begin{bmatrix} 0 & N_1 & 0 & 0 \\ N_2 & N_3 & N_4 & N_5 \\ 0 & N_6 & N_7 & N_8 \\ 0 & N_{10} & 0 & N_{11} \end{bmatrix} \begin{bmatrix} Z_i \\ \dot{X} \\ D_{out}^* \\ U^* \end{bmatrix}, \quad (4)$$

where, $U^* = [U^t\ Y_1^t]^t$. In Eqn. (4), $\dot{X}_i$ depends only on the $\dot{X}$ variables now in derivative causality. Eqn. (4) can also be obtained using the invertible matrix contained in $[S_{11}^t\ S_{21}^t\ S_{31}^t]^t$. Hence, *rank*$([S_{11}^t\ S_{21}^t\ S_{31}^t]^t) = n - t_d$. Finally, we can prove *struct-rank*$([A^t\ C^t]^t) =$ *rank*$([S_{11}^t\ S_{21}^t\ S_{31}^t]^t)$ using the same considerations as in Appendix 1 of [4], but with matrix $[A^t\ C^t]^t$.

The proposed method for analyzing structural observability for linear systems can be extended for nonlinear systems when the nonlinearities can be expressed by making the I, C, and R values as functions of other variables, since the notion of junction structure remains unchanged from that of linear systems. However, this equivalence does not hold when the nonlinearities are linked to the system structure [4].

IV. Factoring DBNs For Efficient Estimation

A. Problem Statement

Given a DBN $D = (\mathbf{X}, \mathbf{U}, \mathbf{Y})$, our goal is to factor D into the *maximal* number of conditionally independent *DBN Factors* (DBN-Fs), $D_i = (\mathbf{X}_i, \mathbf{U}_i, \mathbf{Y}_i)$, $i \in [1, m]$, such that each DBN-F is *observable*. Observability and conditional independence of each DBN-F is a necessary condition for ensuring efficient and accurate state estimates when the estimation algorithm is applied to each DBN-F separately.

Definition 3 (DBN Factor)**.** A *DBN Factor* (DBN-F), $D_i = (\mathbf{X}_i, \mathbf{U}_i, \mathbf{Y}_i)$, $i \in [1, m]$, of DBN $D = (\mathbf{X}, \mathbf{U}, \mathbf{Y})$ is a smaller DBN such that (*i*) $\bigcup \mathbf{X}_i \subset \mathbf{X}$, (*ii*) $\bigcup \mathbf{Y}_i \subset \mathbf{Y}$, (*iii*) $\bigcup \mathbf{U}_i = \mathbf{U} \bigcup (\mathbf{Y} - \cup \mathbf{Y}_i)$, and (*iv*) each D_i is *conditionally independent* from all other DBN-Fs given the inputs, $\mathbf{U}_i$.

Definition 4 (Conditionally Independent DBN-F)**.** Any DBN-F, $D_j = (\mathbf{X}_j, \mathbf{U}_j, \mathbf{Y}_j)$, of a global DBN, $D = (\mathbf{X}, \mathbf{U}, \mathbf{Y})$, is *conditionally independent* from all its other DBN-Fs $D_k = (\mathbf{X}_k, \mathbf{U}_k, \mathbf{Y}_k)$, s.t. $k \neq j, k \in [1, m]$ given $\mathbf{U}_j$ if (*i*) $P(\mathbf{X}_{j_{t+1}} | \mathbf{X}_{t-n:t}, \mathbf{U}_{t-n:t}) = P(\mathbf{X}_{j_{t+1}} | \mathbf{X}_{j_{t-n:t}}, \mathbf{U}_{j_{t-n:t}})$, and (*ii*) $P(\mathbf{Y}_{j_t} | \mathbf{X}_t, \mathbf{U}_t) = P(\mathbf{Y}_{j_t} | \mathbf{X}_{j_t}, \mathbf{U}_{j_t})$.

Definition 5 (Observable DBN-F)**.** A DBN-F, $D_j = (\mathbf{X}_j, \mathbf{U}_j, \mathbf{Y}_j)$ is *observable* if the underlying subsystem it represents is *structurally observable*.

Example: Fig. 2(b) shows four DBN-Fs, $D_1 = (\{f_2, e_3, e_7\}, \{f_9^*\}, \{f_2^*, f_6, e_5\})$, $D_2 = (\{e_{13}\}, \{f_9^*, f_{15}^*\}, \{f_{12}\})$, $D_3 = (\{e_{19}\}, \{f_{15}^*, f_{21}^*\}, \{f_{18}\})$, and $D_4 = (\{e_{25}, f_{27}\}, \{f_{21}^*, F\}, \{f_{24}, f_{27}^*\})$. As shown in Defn. 3, $\cup_{i\in[1,4]}\mathbf{X}_i \subset \mathbf{X}$, $\cup_{i\in[1,4]}\mathbf{Y}_i \subset \mathbf{Y}$, $\cup_{i\in[1,4]}\mathbf{U}_i = \mathbf{U} \cup (\mathbf{Y} - \cup\mathbf{Y}_i)$. Also, each DBN-F shown in Fig. 2(b) is conditionally independent of all other DBN-Fs. For example, in the global DBN shown in Fig. 2(a), the value of variable e_{13} at time step $t+1$ depends

on variables f_9, e_{13}, and f_{15} at time step t, and variables f_2 and e_7, among others, at time step $t-1$, and so on. However, DBN-F, D_2, shown in Fig. 2(b), is conditionally independent of all other DBN-Fs given its inputs f_9^* and f_{15}^* because the values of its state variable, e_{13}, and measurement variable, f_{12}, at time t, do not depend on any variable external to D_2.

B. Overview of Factoring Approach

Our procedure for *factoring* a DBN involves replacing one or more of its state variables by algebraic functions of at most r measured variables, $\mathbf{Y}^r$, where r is a user-specified parameter. Once we express a state variable in terms of $\mathbf{Y}^r$, i.e., $X = g^{-1}(\mathbf{Y}^r)$, considering $\mathbf{Y}^r$ to be inputs, we delete every $X_t \rightarrow X_{t+1}$, $U_t \rightarrow X_{t+1}$, $X_t \rightarrow Y_t$ link, and replace X with $g^{-1}(\mathbf{Y}^r)$. Then, we restore an intra-time slice link $g^{-1}(\mathbf{Y}^r) \rightarrow Y_t$ for every $X_t \rightarrow Y_t$, such that $Y_t \notin \mathbf{Y}^r$. The across-time links into X_t are not restored, since $g^{-1}(\mathbf{Y}^r)$ can be computed independently at each time step. The replacing of sufficient number of state variables in terms of measurements, and the subsequent removal of across-time links involving these state variables produces conditionally independent DBN-Fs.

The goal of our factoring scheme is to generate the maximal number of DBN-Fs that are each observable. A DBN can be factored into maximal number of *observable* DBN-Fs by (*i*) generating maximal number of (possibly unobservable) conditionally independent factors by replacing every state variable which can be determined as an algebraic function of at most r measurements, and (*ii*) merging unobservable DBN-Fs from this maximal factoring into other factors till all of the generated factors are observable.

Example: For the DBN shown in Fig. 2(b), assuming $r = 1$, measurements, f_2^*, f_9^*, f_{15}^*, f_{21}^*, and, f_{27}^*, each depend on the single state variable, f_2, f_9, f_{15}, f_{21}, and, f_{27}, respectively. In this system, f_{15} is directly measured, so $f_{15}^* = g(f_{15})$ trivially exists, and so does the function $h = g^{-1}$. (More generally, a set of measured variables may be needed to establish the value of a state variable, and h will be a function derived from f and g.) Hence, as shown in Fig. 2(b), if we replace f_{15} with the measurement, f_{15}^*, we no longer need variables $f_9, e_{13}, f_{15}, e_{19}$, and f_{21} to compute f_{15}. Thus the across-time links to f_{15} can be removed. So, given the measurement f_{15}^*, the DBN-Fs $D_2 = (\{e_{13}\}, \{f_9^*, f_{15}^*\}, \{f_{12}\})$ and $D_3 = (\{e_{19}\}, \{f_{15}^*, f_{21}^*\}, \{f_{18}\})$ are conditionally independent. Repeating the above procedure and replacing f_9 and f_{21} yields the maximally factored SMD DBN, shown in Fig. 2(b), which contains 4 DBN-Fs. The two middle DBN-Fs in Fig. 2(b) are not observable, since the single state variable in either of the two DBN-Fs does not affect the observed variable. However, the factoring generated by merging each unobservable DBN-F to its observable neighbor (see Fig. 2(c)) results in a factoring where all DBN-Fs are observable.

C. The Factoring Algorithm

Our algorithm for generating maximal number of observable DBN-Fs from a given DBN is as follows: (*i*) partition the DBN into maximal DBN-Fs, (*ii*) map each generated DBN-F to a BG fragment (BG-F) and analyze the structure of this BG-F to determine if the DBN-F is observable, and (*iii*) merge every unobservable DBN-F with other DBN-Fs so as the resultant DBN-Fs may be observable, till all DBN-Fs are observable. These steps (shown in Algorithm 1) are presented in detail below. We assume that the system to be factored is observable, as otherwise, no factoring with only observable factors exist. Also, we assume that we have sufficient sensors to allow factoring.

Algorithm 1 Generating factors of a DBN.

Input: System DBN, D
Generate maximal $Factoring_1 = \{D_1, D_2, \ldots, D_n\}$
$SetOfFactorings = \{Factoring_1\}$
while true do
  $SetOfObsF = \varnothing$; $SetOfUnobsF = \varnothing$;
  for each $Factoring_i \in SetOfFactorings$ **do**
    if every DBN-F in $Factoring_i$ is observable **then**
      $SetOfObsF = SetOfObsF \cup Factoring_i$
    else
      $SetOfUnobsF = SetOfUnobsF \cup Factoring_i$
  if $SetOfObsF \neq \varnothing$ **then**
    $BestFactoring = Factoring_j \in SetOfObsF$ having the most number of balanced DBN-Fs
    exit
  else
    $NextBestFactoring = Factoring_j \in SetOfUnobsF$ having the most number of unobservable DBN-Fs
  $SetOfFactorings =$ all possible pairwise mergings of the DBN-Fs of $NextBestFactoring$

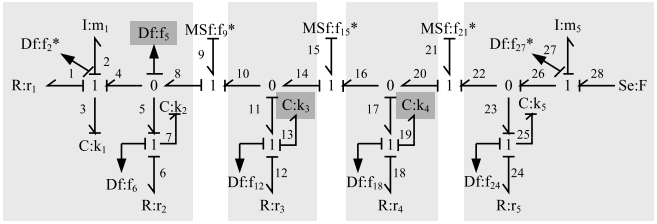

Fig. 4. Four-Factored SMD bond graph with imposed derivative causality.

1) Step 1 - Generating Maximal Factoring: Given the user-specified parameter, r, we analyze the system DBN to identify all state variables that are algebraic functions of single measurements, or pairs of measurements, or triples, and so on, up to r measurements. Then we express these state variables in terms of a subset of measurements, remove the state variables, and all across-time links directed into them. The maximally factored DBN for the SMD system is shown in Fig. 2(b). However, a state variable is not expressed in terms of measurements if the removal of this state variable does not generate any new factors. For example, in Fig. 2(b), f_2 is not replaced with measurement f_2^* since this does not generate any new factors.

2) Step 2 - Testing Observability of DBN-Fs: Given a DBN-F D_i, we can test whether or not it is observable by first mapping D_i to a BG-F, and analyzing this BG-F, B_i for structural observability. Before mapping a D_i to a B_i, we identify the state variables in the global DBN that were removed to generate D_i, and the measurement variables these

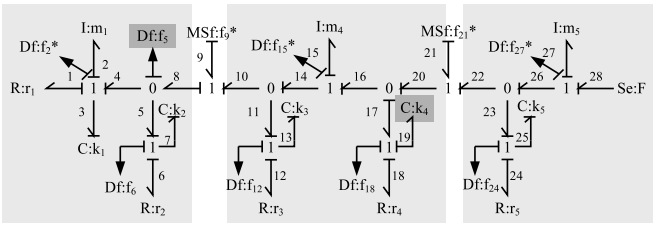

Fig. 5. Three-Factored SMD bond graph with imposed derivative causality.

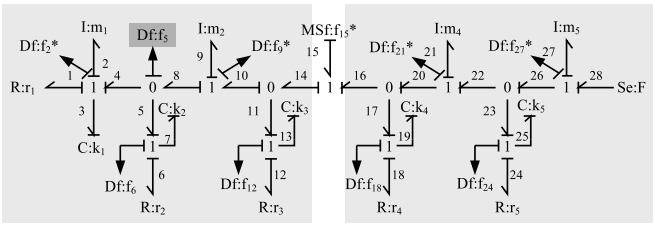

Fig. 6. Two-Factored SMD bond graph with imposed derivative causality.

state variables were replaced with. Given this information, the first step of mapping a D_i to a B_i is to replace the I or C element (in the global BG) corresponding to every state variable that was removed from the global DBN to generate D_i by a MSf or MSe element, respectively, whose value is computed in terms of at most r measurements. Then, we define B_i to be that fragment of the system BG that lies between these newly introduced MSf or MSe elements, as the BG is factored into independent subsystems by these source elements.

Proposition 1. A BG may be factored into *independent* BG factors $B_1, B_2, \ldots, B_n$ by replacing an I or C element with a MSf or MSe element, respectively.

Proof: A capacitor C_1's constituent equation is $e_{C_1} = \frac{1}{C_1}\int f_{C_1}\ dt$. In the state-space formulation, f_{C_1} can be expressed in terms of other state variables. Hence, any measurement or state variable that depends on e_{C_1} would, in turn, be dependent on f_{C_1}, and possibly every other state variable. Now, if f_{C_1} can be measured, and we replace C_1 with modulated $MSe_{C_1} = g^{-1}(f_{C_1})$, the dependence between e_{C_1} and all other state variables is broken, and the BG is factored into *independent* BG-Fs. The proof similarly follows for an I element replaced with a modulated MSf. ■

Example: The maximally factored SMD DBN has four DBN-Fs (Fig. 2(b)), which correspond to the BG-Fs shown in Fig. 4. The two outer BG-Fs are structurally observable, as all their energy storage elements can be assigned preferred derivative causality (albeit by dualizing an effort sensor into a flow sensor, indicated by the shaded background, in the first BG-F), and every state variable affects at least one sensor. The two BG-Fs in the middle, however, are not observable, since, in each of these two BG-Fs, the single state variable does not causally affect the flow sensor. Hence, the maximal DBN factoring shown in Fig. 2(b) cannot be used for accurate state estimation, and some of the factors need to be merged to generate observable DBN-Fs.

3) Step 3 - Merging Unobservable Factors: Unobservable DBN-Fs can be *merged* with other DBN-Fs to generate an observable DBN-F. m DBN-Fs, $D_1, D_2, \ldots, D_m$, can be merged by restoring those state variables and across-time links in the system DBN that were replaced to generate $D_1, D_2, \ldots D_m$. The measurements that were used to compute these state variables are also reintroduced.

Merging an unobservable DBN-F, D_1, with another DBN-F, D_2, results in DBN-F, $D_{1,2}$, which maps to the BG-F, $B_{1,2}$. The merging of D_1 and D_2 results in the replacement of at least one source element in B_1 and B_2 with a I or C element, and reintroduction of at least one sensor element in the resultant $B_{1,2}$. Since, the reintroduced measurement sensors are directly connected to the reinstated I or C elements in $B_{1,2}$, condition 1 of structural observability is satisfied for these reintroduced energy storage elements. Moreover, the new sensor can be causally linked to other I or C elements that are not linked to any sensor element, further aiding the satisfaction of condition 1 for $B_{1,2}$. Also, the greater are the number of sensors in $B_{1,2}$, the greater is the flexibility for dualizing these sensors to satisfy condition 2.

Algorithm 1 shows how the merging procedure is invoked if a DBN-F in the maximally factored DBN is not observable. In each iteration of this algorithm, we create new factorings through all possible pairwise mergings of unobservable DBN-Fs, to create at least one new factoring with all its DBN-Fs observable. When multiple factorings are generated, we use a heuristic to choose that factoring which has the most number of *balanced* DBN-Fs with respect to state variables. If the merging step does not generate any factorings with all its DBN-Fs observable, we select the maximal factoring with the largest number of factors and highest number of unobservable DBN-Fs, and generate the next set of factorings by pairwise merging of unobservable DBN-Fs. This procedure is repeated till we obtain at least one factoring where all the DBN-Fs are observable. Since the system was initially observable, continued merging will eventually result in a factoring in which all DBN-Fs are observable, at worst producing the original DBN model. Therefore, our factoring algorithm terminates.

Example: The unobservable DBN-Fs, shown in Fig. 2(b), can be merged in two possible ways to form two different factorings. The factoring shown in Fig. 5 corresponds to a DBN-F generated by merging the two central DBN-Fs, and is not unobservable (since capacitor k_4 does not provide a consistent causal assignment when it is assigned derivative causality). However, the two BG-Fs shown in Fig. 6, and corresponding to the DBN-Fs shown in Fig. 2(c), are observable, and hence, we select this as our desired factoring.

D. Tracking using Factored DBNs

Given m observable DBN-Fs, $D_1, D_2, \ldots, D_m$, we can implement an inference algorithm on each DBN-F as an independent process. For our work, we implemented m PFs, one for each DBN-F. Each PF takes as inputs, $\mathbf{U}_i$, and estimates $\mathbf{X}_i$ based on $\mathbf{Y}_i$. Only measurements $\bigcup_i \mathbf{U}_i$ are communicated between PFs. The PF for the DBN-F D_i uses

$a\frac{|\mathbf{X_i}|}{|\mathbf{X}|}$ particles, where a is a user-specified parameter. For m DBN-Fs, $\sum_i |\mathbf{X_i}| < |\mathbf{X}|$, where $\mathbf{X}$ is the total number of states in the complete system. Therefore, the complexity of tracking using each DBN-F is less than that of tracking using the global DBN. Also, since the inference algorithms on the different factors are executed simultaneously, the total complexity of inference reduces to the complexity of the PF with the maximum number of particles.

V. Experimental Results

For our experiments, we assumed all probability distributions to be Gaussian, and all sensors to have white Gaussian noise with 0 mean and power 1 dbW. We estimated the state variables using the DBN factorings shown in Fig. 2(c) for 10 runs. Given m DBN-Fs, $D_i = \{\mathbf{X}_i, \mathbf{U}_i, \mathbf{Y}_i\}$, $i = 1, 2, \ldots, m$, such that $\mathbf{X} = \mathbf{X}_1 \cup \mathbf{X}_2 \cup \ldots \mathbf{X}_m$, for each run we computed the estimation error: $E = \frac{1}{|\mathbf{X}|}\sum_{X\in\mathbf{X}}\left(\frac{1}{T}\sum_{t=0}^{T}(X_t - X_t^{model})^2\right)$, where T is the total simulation time, X_t denotes the estimated value of state X at time t, and X_t^{model} denotes the actual value of state X at time t obtained from the simulation model. Table I reports the mean and standard deviation of errors obtained from each factoring over all runs.

To demonstrate that the factoring scheme preserves the system dynamics, we hypothesized the difference in errors for the 2-factor and unfactored DBN would not be statistically significant, and the error for the 4-factor DBN would be significantly larger than the unfactored DBN. Further the difference in error for the 2-factor and 4-factor DBNs would also be statistically significant. We ran t-tests to establish significance of the differences. The tests for significance indicated that the errors obtained using the 2-factor DBN did not significantly differ from that obtained using the unfactored DBN ($p < 0.05$), while those obtained using the 4-factor DBN was significantly greater ($p < 0.05$). The test of significance between the 2- and 4-factor DBN showed that the error in the 4-factor DBN was significantly larger ($p < 0.05$). Therefore, the 2-factor DBN preserves dynamics of the unfactored DBN, whereas the 4-factor DBN, which has unobservable factors, does not.

Table II shows the average time taken by the slowest PF for each factoring to track system behavior for 1500 time steps. The time taken by a PF depends on the number of particles it uses. In our experiments, the number of particles used by a PF was proportional to the number of states in the DBN factor the PF was associated with. Hence, PF for unfactored DBN (with 1000 particles) took the most time, followed by the PF on the larger DBN-F of the 2-factor DBN (with 500 particles). The least amount of time was taken by the PFs applied to the 4-factor DBN, since its largest DBN-F has 3 state variables, and hence, its PF used 300 particles.

TABLE I

Estimation errors averaged over 10 runs

No. of Factors →	1	2	4
Mean	0.1143	0.1381	0.1968
(Standard Deviation)	(0.0360)	(0.0470)	(0.0314)

TABLE II

Time taken for particle filter to complete estimation

No. of Factors →	1	2	3	4
Time (s)	137.03	37.74	18.79	18.97

VI. Discussion and Conclusions

This paper presented an approach for factoring DBNs based on structural observability. Each of the DBN factors are conditionally independent from all other factors given the measurements that are communicated between them, thus preserving the dynamics of the global system behavior. Experimental results showed that factoring maintains inference accuracy in DBNs while improving the efficiency of DBN inference in the presence of sensor noise. Future work will focus on evaluating inference accuracy in the presence of sensor faults. In particular, we need to evaluate the effect on inference caused by faults in sensors that decouple two or more DBN-Fs. Our intuition is that the presence of a fault in such a sensor will affect the estimation accuracy of the state variables in only those factors which uses this sensor as an input. The estimation accuracy of state variables in other factors will remain unaffected by this sensor fault, since each factor is conditionally independent given the measurements used as system inputs.

References

[1] K. P. Murphy, "Dynamic Bayesian networks: Representation, inference, and learning," Ph.D. dissertation, University of California, Berkeley, 2002.

[2] X. Boyen and D. Koller, "Tractable inference for complex stochastic processes," in *Proc. of the* 14^{th} *Annual Conference on Uncertainty in Artificial Intelligence*, 1998, pp. 33–42.

[3] D. Koller and U. Lerner, "Sampling in factored dynamic systems," in *Sequential Monte Carlo Methods in Practice*, A. Doucet, N. de Freitas, and N. Gordon, Eds. Springer, 2001.

[4] C. Sueur and G. Dauphin-Tanguy, "Bond graph approach for structural analysis of MIMO linear systems," *Journal of the Franklin Institute*, vol. 328, no. 1, pp. 55–70, 1991.

[5] ——, "Structural controllability/observability of linear systems represented by bond graphs," *Journal of The Franklin Institute*, vol. 326, no. 6, pp. 869–883, 1989.

[6] A. Mutambara, *Decentralized Estimation and Control of Multisensor Systems*. CRC Press, 1998.

[7] C. Frogner and A. Pfeffer, "Discovering weakly-interacting factors in a complex stochastic process," in *Advances in Neural Information Processing Systems 20*, J. Platt, D. Koller, Y. Singer, and S. Roweis, Eds. Cambridge, MA: MIT Press, 2008, pp. 481–488.

[8] B. Ng and L. Peshkin, "Factored particles for scalable monitoring," in *In Proceedings of the Eighteenth Conference on Uncertainty in Artificial Intelligence*. Morgan Kaufmann, 2002, pp. 370–377.

[9] U. Lerner, R. Parr, D. Koller, and G. Biswas, "Bayesian fault detection and diagnosis in dynamic systems," in *Proc. of Seventeenth National Conference on Artificial Intelligence*, 2000, pp. 531–537.

[10] P. J. Mosterman and G. Biswas, "Diagnosis of continuous valued systems in transient operating regions," *IEEE-SMCA*, vol. 29, no. 6, pp. 554–565, 1999.

[11] D. C. Karnopp, D. L. Margolis, and R. C. Rosenberg, *Systems Dynamics: Modeling and Simulation of Mechatronic Systems*, 3rd ed. New York, NY, USA: John Wile & Sons, Inc., 2000.

[12] M. S. Arulampalam, S. Maskell, N. Gordon, and T. Clapp, "A tutorial on particle filters for online nonlinear/non-gaussian bayesian tracking," *IEEE Trans. on Signal Processing*, vol. 50, no. 2, pp. 174–188, 2002.

[13] A. K. Samantaray and B. O. Bouamama, *Model-based Process Supervision: A Bond Graph Approach*. Springer, 2008.